COMPGV19: Assignment 2: Subsampled MRI

Antonio Remiro Azócar, MSc Machine Learning

20 March 2017

Introduction

Magnetic Resonance Imaging (MRI) is an essential modality in medical imaging but suffers from very slow data acquisition times. Such lack of speed is intrinsic, primarily attributed to physical (e.g. magnetic field amplitudes limiting gradients) and physiological (e.g. peripheral nerve stimulation) constraints [1]. Compressed sensing seeks to speed up acquisition times by sampling below the Nyquist rate. This introduces artifacts which require computationally intensive image reconstruction to be removed.

Background and Mathematical Formulation

In MRI, magnetic pulse sequences produce signal intensities which are received by RF coils. Such intensities provide an image contrast. The ***k*-space** trajectory of the MR pulse sequence is the domain of data acquisition. It contains information on spatial frequencies and is mapped to the image domain by a Fourier transformation [1]. The data to populate the k-space matrix is taken directly from the MR signals, their location in the matrix relating to their magnetisation distribution (lower spatial frequencies are at the center and increase while moving away from it).

MR image reconstruction aims to visualize $m(\overrightarrow{r})$, the transverse magnetisation at spatial coordinates $\overrightarrow{r}$. The RF coils measure a signal $s(t)$ concealed by a linear phase, with the Fourier integral form:

$$s(t) = \int_{\mathbb{R}^d} m(\overrightarrow{r}) e^{-i2\pi \overrightarrow{k}(t)\cdot\overrightarrow{r}(t)} d\overrightarrow{r} = F(\overrightarrow{k}(t)), \tag{1}$$

In essence, we have an **inverse problem** where $s(t) = F(\overrightarrow{k}(t))$ is the Fourier transform of the unknown magnetisation $m(\overrightarrow{r})$ sampled at spatial frequency $\overrightarrow{k}(t)$. We measure noisy Fourier coefficients $F(\overrightarrow{k}(t))$. Note the measured MR signal y_i differs from the true signal $s(t_i)$ due to the presence of measurement noise ϵ_i ($y_i = s(t_i) + \epsilon_i$, $i = 1, ..., M$ for M measurements). $e^{-i2\pi \overrightarrow{k}(t)\cdot\overrightarrow{r}(t)}$ provides the problem's spatial information.

In an image **acquisition**, a magnetisation $m(\overrightarrow{r})$ is sampled at a given k-space trajectory. The data from a series of acquisitions reconstructs the MR image. However, notice that while the recorded measurements $y = y_1, ..., y_M$ are finite, the $m(\overrightarrow{r})$ we wish to find is a continuous-space function. We thereby encounter a problem which is underdetermined and has no canonical solution, providing only 'partial' k-space data. Consider a continuous-continuous formulation ($m(\overrightarrow{r})$ and $s(t)$ treated continuously) of (1). Provided with a 'continuum' of signal measurements, (1) can be solved via an inverse Fourier transform. We have the **forward formulation**:

$$m(\overrightarrow{r}) = \int_{\mathbb{R}^d} F(\overrightarrow{k}(t)) e^{i2\pi \overrightarrow{k}(t)\cdot\overrightarrow{r}(t)} d\overrightarrow{k}. \tag{2}$$

Subsampling Schemes (I)

The partial data problem can be solved by devising a sampling pattern, designing k-space trajectories for each acquisition. Such pattern may be designed to meet the Nyquist criterion [2], which sets the required coverage of the k-space. Undersampling k-space data (attempting to reduce imaging speed) results in a violation of the Nyquist criterion, with Fourier reconstructions exhibiting aliasing artifacts.

Discretising the integral solution in equation (2), we obtain:

$$\hat{m}(\overrightarrow{r}) = \sum_{i=1}^{M} F(\overrightarrow{k}_i(t)) e^{i2\pi \overrightarrow{k}_i(t)\cdot\overrightarrow{r}(t)} \approx \sum_{i=1}^{M} y_i w_i e^{i2\pi \overrightarrow{k}_i(t)\cdot\overrightarrow{r}(t)}, \tag{3}$$

where weights w_i are 'sampling density correction factors'. Perhaps the most popular trajectory design involves sampling **straight lines from a cartesian grid**. For **cartesian sampling**, it is sufficient to choose $w_i = \frac{1}{N}$ in (3). This reduces the expression to an inverse Fast Fourier Transform, making image reconstruction simple.

This inherent simplicity, along with the robustness of reconstructions [2], are reasons for the popularity of cartesian pulse sequences in medical imaging.

For **non-cartesian sampling**, k-space trajectory design may involve sampling along **radial lines** or along **spiral trajectories**. Fast reconstruction from the aforementioned trajectories involves using interpolation (e.g. **gridding**) [3] or filtered back-propagation schemes instead of summation. Sampling along radial lines provides less sensitivity to motion artifacts than cartesian trajectories. This sampling scheme allows for undersampling [4], particularly when dealing with images of high contrast [5]. Sampling along spiral trajectories is also widely popular in medical imaging, allowing for efficient utilisation of the gradient system hardware [6]. Non-cartesian schemes may be highly susceptible to system imperfections.

An Introduction to Compressed Sensing

We previously made reference to the physical and physiological constraints limiting the speed at which k-space is traversed. 'Compressed sensing' (CS) groups techniques seeking to exploit sparsity, more explicitly **transform sparsity**, in the k-means data. Transform sparsity is inherent to MRI and is a fairly general concept, relating to the sparse representation of the image we wish to reconstruct in a transform domain. A more formal definition of sparsity is provided by S-sparsity. A signal is S-sparse if at most S of its coefficients can be non-zero. This reduces the signal's degrees of freedom to S, requiring a number of measurements proportional to its compressed rather than its uncompressed size to be reconstructed. This is the fundamental philosophy of CS techniques, which fit well with MRI for the following reasons:

- **Medical images are intrinsically sparse**, either in the image domain e.g. angiograms (sparsity in the identity transform), or in other domains; e.g. the wavelet domain (brain images) or in a domain of spatial finite differences [7].
- **Medical images are naturally compressible**: They can be compressed with little loss of visual information via sparse coding (e.g. discrete cosine transform, wavelet transform) in an adequate domain.
- **MRI scanners acquire spatial-frequency encoded data**; instead of pixel samples in the image domain.

An MR image can be reconstructed via compressed sensing provided three conditions are satisfied [9]:

- The image **exhibits transform sparsity** and is therefore compressible via transform coding.
- **Aliasing artifacts** in the transform domain resulting from k-space subsampling are **incoherent** (noise-like).
- An adequate **non-linear recovery scheme** (one which preserves sparsity) is utilised to reconstruct the image.

The first condition has already been discussed. The second condition concerns choosing an appropriate subset of the k-space domain; one which allows for efficient noise-like sampling of trajectories.

Subsampling schemes (II)

Early CS research [8] [9] sampled completely random k-space subsets. This approach was adopted to guarantee extremely low coherence and mathematical simplicity. However, it is impractical in all dimensions [2] [7]; primarily because it does not result in reasonably smooth curves/lines. This is problematic due to physiological and hardware limitations. Random point k-space sampling also lacks the robustness to withstand non-toy situations and does not account for the non-uniform distribution of energy in MRI's frequency domain. We must avoid focussing on 'optimising' incoherence and settle for a scheme which partially replicates the irregularity of pure random subsampling while allowing for rapid data acquisition. Such scheme should ideally provide realistic energy distributions, with higher density sampling close to the k-space center and decaying sampling rates towards the periphery. [10], [11] and [12] propose the non-uniform cartesian subsampling of series of acquisitions as a suitable scheme. This implementation is simple and provides incoherent artifacts. In addition, data acquisition times are low, with scan time reductions proportional to the level of undersampling, and randomness is attained in the phase-encode dimensions.

Comparing k-space trajectory designs. Point Spread Function (PSF) and Transform Point Spread Function (TPSF) analyses provide a systematic way of measuring incoherence. Consider first an image with sparsity in the image domain. Let F_S denote the undersampled Fourier operator; that computed only at frequencies in a sampled subset S of k-space. The PSF of the image is given by:

$$\mathrm{PSF}(i,j) = e_j^* F_S^* F_S e_i, \tag{4}$$

where F_S^* is the adjoint of F_S and e_i is the ith vector of the natural basis. As discussed previously, most MR images of interest show sparsity in a different transform domain than the image domain. TPSF analysis extends the concept of PSF to measure incoherence for such images. We have,

$$\text{TPSF}(i,j) = e_j^* \Psi F_S^* F_S \Psi^* e_i, \tag{5}$$

where Ψ is an orthogonal sparsifying transform mapping the pixel domain to the new transform domain. A formal measurement of coherence is given by $\max_{i \neq j} = |\text{TPSF}(i,j)|$ i.e. the off-diagonal entry of greatest magnitude of the TPSF. We wish to select a subsampling scheme with noise-like statistics and the lowest TPSF possible.

More sophisticated subsampling schemes. [7] proposes a Monte-Carlo design method to find a coherence-minimising subsampling scheme. It proceeds as follows:

1. Select a grid size subject to the FOV and resolution required.
2. Formulate a probability density function (pdf) and take values from it to undersample the grid.
3. The pdf structure determines k-space variable-density sampling. Reduce density per a power of distance to the k-space origin.
4. To avoid selecting a scheme with a 'poor' TPSF, iterate the method multiple times, keeping track of the run giving the greatest $\max_{i \neq j} = |\text{TPSF}(i,j)|$.
5. Select the scheme with lowest peak interference and if necessary, store for future scans.

This 'random' procedure is appropriate given that we are dealing with a (perhaps intractable) combinatorial optimisation problem. Other acceleration methods have been suggested in recent literature. [20] suggests undersampling k-space and applying a Bayesian reconstruction to randomised trajectories.

Image reconstruction: An optimisation problem

Compressed sensing: Ax=b revisited. In this case, A is a Fourier matrix and the problem is underdetermined. **The ℓ^2 norm.** For this problem, the least squares solution, $x^* = \text{argmin}_{x:Ax=b} ||x||_{\ell^2} = A^T(AA^T)^{-1}b$, is not appropriate. When reconstructing the image from partial Fourier coefficients, the least squares solution is a partial Fourier series which may differ greatly from the original signal.

The ℓ^0 norm. It can be proved that an S-sparse signal x can be reconstructed uniquely from Ax, provided with the linear independence of any $2S$ columns of A [14]. Relating to image reconstruction: if the image of interest is a vector m and Ψ is the sparsifying transform (in which Ψm is sparse), our reconstruction can be achieved by:

$$\text{minimising} \quad ||\Psi m||_{\ell^0} = \#(i|[\Psi m]_i \neq 0). \tag{6}$$

Here $||\Psi m||_{\ell^0}$ represents the sparsity of Ψm; we are trying to find the unique sparsest solution to the problem. In comparison to least-squares estimation, ℓ^0 minimisation is intractable computationally, it is generally NP-hard and it is not a convex optimisation problem.

The ℓ^1 norm. ℓ^2 minimisation, while being simple to compute is often incorrect for underdetermined systems. ℓ^0 minimisation, while being often correct is computationally intractable. ℓ^1 minimisation gives us the best of both worlds, attaining image reconstruction via:

$$\text{minimising} \quad ||\Psi m||_{\ell^1} = \sum_i |[\Psi m]_i|. \tag{7}$$

ℓ^1 minimisation has the advantage of being a convex optimisation problem which can be solved reasonably quickly [14]. In addition, it often results in a sparse solution, it is robust to noise and has been proved to guarantee near-optimal performance provided there is sufficient incoherence [8] [14]. ℓ^2 minimisation gives greater penalties to larger coefficients, giving solutions with many small coefficients which are not sparse. In ℓ^1 minimisation, many small coefficients bear a larger penalty than only a few large coefficients. This promotes a sparse solution, restraining the presence of smaller coefficients.

[2] and [7] provide the following recovery scheme for image reconstruction:

$$\begin{aligned} &\text{minimising} \quad ||\Psi m||_{\ell^1}, \\ &\text{s. t.} \quad ||F_S m - y||_{\ell^2} < \epsilon. \end{aligned} \tag{8}$$

Here, y is the k-space data measured by the scanner and ϵ is a threshold parameter enforcing consistency between the reconstructed image and the k-means measurements. ϵ is usually assigned a value roughly below the noise level. The constraint guarantees a solution which is compressible by Ψ.

Total-Variation. When the transform domain is sparse in terms of spatial finite differences, the objective function in (8) is the sum of absolute deviations in m. In this case, the objective function is denoted as $TV(m)$ (Total-Variation) [15]. An alternative formulation of (8) accounting for $TV(m)$ is:

$$\begin{aligned} \text{minimising} \quad & ||\Psi m||_{\ell^1} + \alpha TV(m), \\ \text{s. t.} \quad & ||F_S m - y||_{\ell^2} < \epsilon, \end{aligned} \tag{9}$$

Here, both the sparsity of Ψ and that of finite differences are promoted. [7] also proposes a formulation accounting for **prior knowledge of phase variation**. Low-order phase variation is triggered by instrumental phase errors in MRI. This makes images harder to sparsify, particularly in the finite difference domain. Phase variations can be estimated by utilising completely sampled k-space data at low resolution. Alternatively, one can estimate the low-order phase by solving (8), then repeating the reconstruction via,

$$\begin{aligned} \text{minimising} \quad & ||\Psi m||_{\ell^1}, \\ \text{s. t.} \quad & ||F_S P m - y||_{\ell^2} < \epsilon, \end{aligned} \tag{10}$$

where P is a diagonal matrix with elements representing phase estimations for each pixel. In (10), the image can be restricted to be real. This approach integrates CS with phase-constrained partial k-space. In essence, **any type of prior knowledge which can be formulated as a convex constraint can be included**.

An active area in current research involves finding fast reconstruction algorithms to solve the aforementioned objective functions. Procedures proposed include using homotopy [17] and iteratively re-weighted least squares [18].

Parallel MRI

Parallel RF coils can be utilised to give a more involved forward model, exploiting redundancies in the k-space by design instead of by sparsity. Using an array of receiver coils provides more effective data per acquisition resulting in lesser acquisitions per scan. There exist ***k*-space domain** (e.g. SMASH) and **image domain** (e.g. SENSE) image reconstruction methods. Whereas the first reconstruct artifact-free images directly from the aliased images, the latter do so from undersampled k-means data.

SENSE (Sensitivity-Encoded) Reconstruction: Consider the model:

$$s(t) = \int_{\mathbb{R}^d} m(\overrightarrow{r}) s^{coil}(\overrightarrow{r}) e^{-i2\pi \overrightarrow{k}(t)\overrightarrow{r}(t)} d\overrightarrow{r}. \tag{11}$$

SENSE reconstruction introduces the term $s^{coil}(\overrightarrow{r})$ to the model in (1). This term represents the receiver coil sensitivity patterns. The goal is to reconstruct $m(\overrightarrow{r})$ given sensitivity maps $s^{coil}(\overrightarrow{r})$. SENSE reconstruction can be combined with CS by accounting for coil sensitivity information in the objective function in (8). Similarly, CS and/or SENSE can be combined with other models to capitalise on other redundancies. For example, we can include the term $e^{-i\omega(\overrightarrow{r})t}$, where $\omega(\overrightarrow{r})$ is an off-resonance frequency map, to introduce a field-inhomogeneity correction. [13] discusses other model-based approaches.

Appendix

Data visualisation

What does the data look like? An open MRI dataset of knee images has been downloaded from `mridata.org` [19]. The dataset was originally provided by Prof. M. Lustig and Dr. S. Vasanawala and was acquired on a GE clinical 3T scanner at Stanford's Lucille Packard Children's Hospital. It consists of 320×320 (2D k-space) $\times 256$ (number of slices) $\times 8$ (number of channels) **fully sampled** raw k-space data in 4D complex double format. Images for each slice are reconstructed by taking an inverse Fourier transform over the entire k-space and combining all 8 channels via sum of squares. Figure 1 presents a plot of real-imaginary values of k-space data for slice 167 (only channel 1 for simplicity). This is our domain of data acquisition. Figure 2 presents the image reconstructed from such slice after merging all channels.

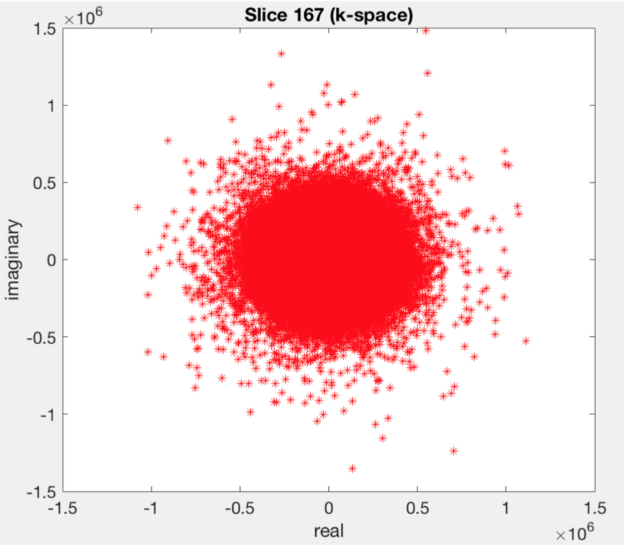

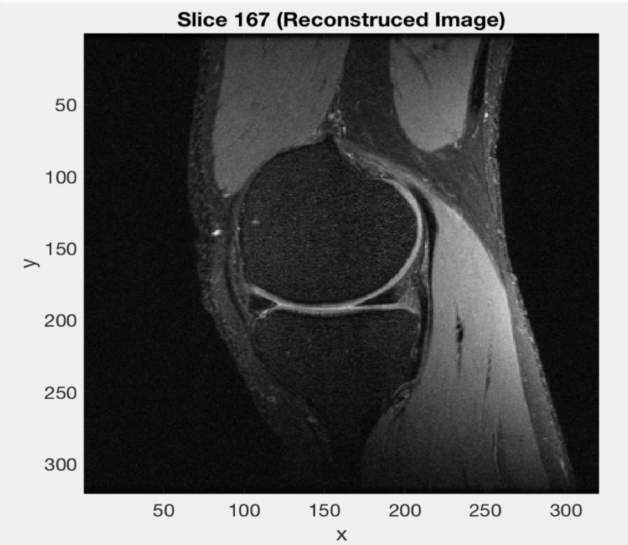

Figure 1 (left): Plot of the k-space data for slice 167, channel 1. Figure 2 (right): Knee image reconstructed for slice 167 using the inverse Fourier transform.

`mridata.org` also provides undersampled datasets (variable-density and uniform-density). These will be of greater interest when implementing our reconstruction algorithms. Note the fully sampled datasets can also be utilised to test our own undersampling patterns.

References

[1] G. Wright. Magnetic Resonance Imaging. *IEEE Signal Processing Mag*, 14(1), pp. 56-66, Jan. 1997.
[2] M. Lustig, D. L. Donoho, J. M. Santos, and J. M. Pauly. Compressed Sensing MRI. *IEEE Signal Processing Magazine*, 25(2): pp. 72–82, March 2008.
[3] J.I. Jackson, C.H. Meyer, D.G. Nishimura, and A. Macovski. Selection of a convolution function for Fourier inversion using gridding. *IEEE Trans. Med. Imag.*, 10(3): pp. 473–478, 1991.
[4] K. Scheffler and J. Hennig. Reduced circular field-of-view imaging. *Magn. Reson. Med.*, 40(3): pp. 474–480, 1998.
[5] D.C. Peters, F.R. Korosec, T.M. Grist, W.F. Block, J.E. Holden, K.K. Vigen, and C.A. Mistretta. Undersampled projection reconstruction applied to MR angiography. *Magn. Reson. Med.*, 43(1): pp. 91–101, 2000.
[6] C.H. Meyer, B.S. Hu, D.G. Nishimura, and A. Macovski. Fast spiral coronary artery imaging. *Magn. Reson. Med.*, 28(2): pp. 202–213, 1992.
[7] M. Lustig, D. Donoho, and J. M. Pauly. Sparse MRI: The application of compressed sensing for rapid MR imaging. *Magnetic Resonance in Medicine*, 58(6): pp. 1182– 1195, 2007.
[8] E. Candès, J. Romberg, and T. Tao. Robust uncertainty principles: Exact signal reconstruction from highly incomplete frequency information. *IEEE Trans. Inform. Theory*, 52(2): pp. 489–509, 2006.
[9] D. Donoho. Compressed sensing. *IEEE Trans Inf Theory*, 52: pp. 1289–1306, 2006.
[10] G.J. Marseille, R. de Beer, M. Fuderer, A.F. Mehlkopf, D. van Ormondt. Nonuniform phase-encode distributions for MRI scan time reduction. *J Magn Reson*, 111: pp. 70–75, 1996.
[11] C.M. Tsai, D. Nishimura. Reduced aliasing artifacts using variable-density k-space sampling trajectories. *Magn Reson Med*, 43: pp. 452–458, 2000.
[12] A. Greiser, M. von Kienlin. Efficient k-space sampling by density-weighted phase-encoding.*Magn Reson Med*, 50: pp. 1266–1275, 2003.
[13] J.A. Fessler. Mathematical challenges in magnetic resonance imaging.[PowerPoint presentation]. *SIAM Conference on Imaging Science*. 2008. Available from: http://web.eecs.umich.edu/ fessler/papers/files/talk/08/ siam-plenary.pdf [Accessed 18 March 2016].
[14] T. Tao. Compressed sensing: or the equation $Ax = b$ revisited. [PowerPoint presentation]. *University of California, Los Angeles*. 2010. Available from: http://www.math.hkbu.edu.hk/ ttang/UsefulCollections/compressed-sensing1.pdf [Accessed 18 March 2016].
[15] L. Rudin, S. Osher, E. Fatemi. Non-linear total variation noise removal algorithm. *Phys. D*, 60: pp. 259–268, 1992.
[16] T.C. Chang, L. He, T. Fang. MR image reconstruction from sparse radial samples using bregman iteration. In: Proceedings of the 13th Annual Meeting of ISMRM, p. 696. Seattle, 2006
[17] D. Donoho et. al, Fast solution of ℓ^1 minimization where the solution may be sparse, Statistics Department, Stanford University, technical report #2006-18, 2006.
[18] J.C. Ye, S. Tak, Y. Han, H.W. Park. Projection reconstruction MR imaging using FOCUSS. *Magn Reson Med*, 57: pp. 764–775, 2007.
[19] MRI Data: MR Datasets for Compressed Sensing. Available from: http://mridata.org [Accessed 18 March 2016].
[20] F. Wajer. Non-Cartesian MRI Scan Time Reduction through Sparse Sampling. PhD thesis, Delft University of Technology, 2001.